Image Processing Techniques for the Numerology Analysis

Che-Wei Chang[#1], Shan-Kun Tien[#2], Shu-Heng Chang[#3], Cheng-Yuan Chang[#4]

Department Of Electrical Engineering, National United University
2, Lienda, Miaoli 36063, Taiwan, R.O.C.

[1]jay30613@gmail.com
[2]akein6230@hotmail.com
[3]vvvv5109@yahoo.com.tw
[4]chengyuan@nuu.edu.tw

***Abstract*— In the traditional facial numerology analysis, it is necessary for the people to analyze the characteristics of personality by observing the facial features by themselves, thus it seems to be inconvenient and time-consuming a little bit. In this paper, a facial numerology analysis system which utilizes image processing techniques instead of the traditional facial recognition by people is proposed. The proposed system is implemented by simply using a camera, MATLAB program and image processing techniques to perform the facial recognition and numerology analysis quickly.**

***Keywords*— Image processing, facial recognition, numerology analysis.**

1. INTRODUCTION

With the rapid evolution of digital image processing techniques, several biometric authentication applications, such as facial recognition, speech recognition, fingerprint recognition, iris recognition, and so on, have been provided for the human beings with the greater convenience and reliability [1]–[4]. The facial recognition is one of the most popular biometric authentication techniques because of several advantages, such as contactless and non-invasive properties during the detection process, compared to the fingerprint recognition and iris recognition [4].

It seems to be inconvenient and time-consuming a little bit when people do the traditional facial numerology analysis. It is because that they have to observe the facial features by themselves in order to analyze the characteristics of personality in accordance with the observations. In this paper, a facial numerology analysis system which utilizes image processing techniques instead of the traditional facial recognition by people is proposed. The proposed system can automatically provide the facial feature recognition by using a camera, MATLAB program and image processing techniques, and then it can perform the facial numerology analysis in accordance with the results quickly.

The organization of the rest of the paper is as follows. In Section 2, the basic theories of image processing techniques are introduced and studied briefly. The study and design process of the proposed system are illustrated in Section 3. Experiment results of the proposed system are presented in Section 4. Finally, conclusions are drawn in Section 5.

2. BASIC THEORIES OF IMAGE PROCESSING TECHNIQUES

2.1. Gray Level

A color space, so-called a color model, is a mathematical representation which simply describes the range of colors as tuples of numbers (e.g., RGB) [5]. Fig. 1 illustrates the RGB color space as an RGB color cube, in which the vertices are the primary (i.e., red (R), green (G), and blue (B) color) and the secondary (i.e., cyan (C), magenta (M), and yellow (Y)) colors, respectively [1]. In general, the red, green and blue colors are called as the three images forming an RGB color

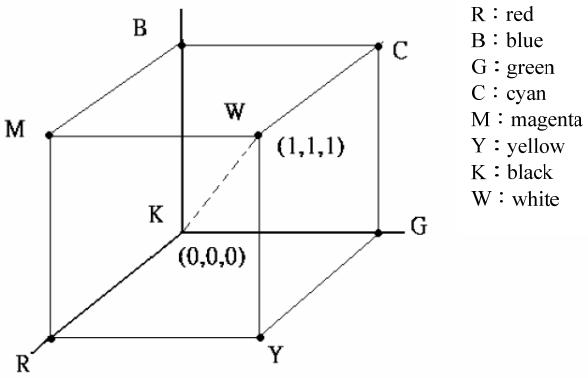

Fig. 1 RGB color space [1].

(a) (b)

Fig. 2 (a) 24-bit RGB image; (b) Gray-level version of (a) obtained, based on Eq. (1).

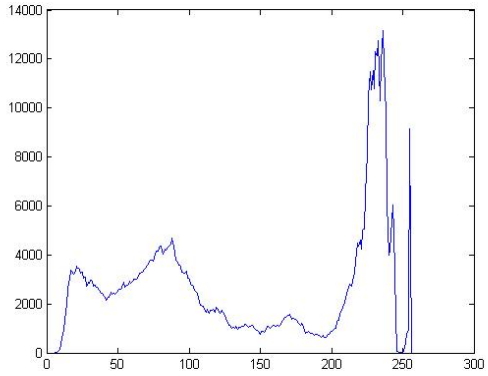

Fig. 3 Histogram of gray-level image in Fig. 2(b).

image. The range of value of the component images is [0, 255] for RGB images of class unit8 [6]. However, if all component images are identical, the result becomes a gray-level image. The definition of "gray level" is to transfer a full-color image (i.e., 24-bit RGB image) into the gray-level image, based on the following equation [7], [8].

$$GRAY = 0.299 \times R + 0.587 \times G + 0.114 \times B \quad (1)$$

Fig. 2(a) shows the original 24-bit RGB image and Fig. 2(b) illustrates the gray-level version of (a) obtained, based on Eq. (1). It should be noted that the effects of dithering are usually better illustrated with gray-level images after comparing with both Fig. 2(a) and (b).

2.2. Histogram

The histogram of the gray-level image mainly consists of it gray levels, which means a graph indicting the number of times each gray level occurs in the gray-level image [6], [9]. That is, the horizontal axis of the graph represents the gray levels (i.e., 0~255), and the vertical axis represents the number of pixels in the particular level. In general, the image histograms can be useful tools for thresholding, because the information in the graph is a representation of pixel distribution which can be analyzed and used for the image processing applications, such as the edge detection, image segmentation, and so on, by setting a appropriate threshold value [5], [6], [9]. Fig. 3 shows the histogram of the gray-level image in Fig. 2(b).

(a) (b)

Fig. 4 (a) Binary image when threshold T=60; (b) Binary image when threshold T=0.

2.3. Binary

For the image processing and identification, we sometimes only require some gray level values, such as black and white colors, thus the image binarization is an extreme approach to strengthen the contrast of the image. In general, the gray-level image will be converted into binary image by using the critical value method which decides a threshold in accordance with the histogram. Then, the binary image $g(x,y)$ can be defined as follows [5], [6], [10]:

$$g(x,y) = \begin{cases} 0, & \text{if} \quad f(x,y) > T. \\ 1, & \text{otherwise.} \end{cases} \quad (2)$$

where $f(x,y)$ is the original gray-level image, and T denotes the threshold which is decided, based on the histogram. If $g(x,y) = 1$, which represents black color, on the contrary, it represents white color when $g(x,y) = 0$. Binary images with different thresholds are shown in Fig. 4(a) (i.e., T=60) and (b) (i.e., T=0), respectively.

2.4. Skin Color Detection

In order to reduce the color for the dependence on the light source, we convert the color image from RGB color space to normalized color coordinates (NCC) color space, because the RGB image is sensitive to the external light source. Then, the normalized components of red and green colors, r and g, which can mainly lower the dependence on the light source, and the parameter of W can be obtained as [5], [6]

$$r = \frac{R}{R+G+B} \quad (3)$$

$$g = \frac{G}{R+G+B} \quad (4)$$

and

$$W = (r - 0.33)^2 + (g - 0.33)^2, \quad (5)$$

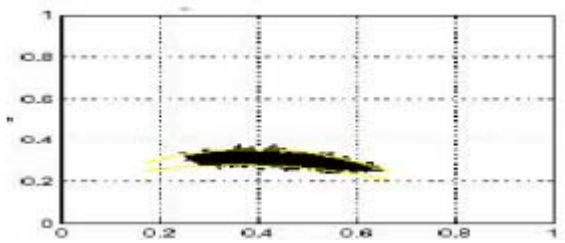

Fig. 5 Statistic chart of skin color.

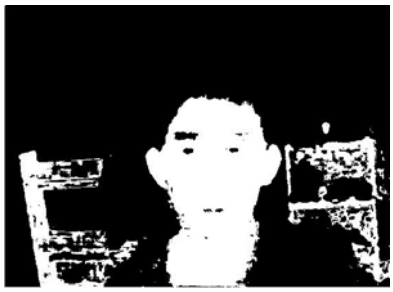

Fig. 6 The image after skin color detection.

respectively. According to Eqs. (3)-(5), the skin color detection of the color image can be evaluated as following equations [11], [12].

$$S = \begin{cases} 1, \text{ if } (g < f_1(r)) \,\&\, (g < f_2(r)) \,\&\, (W > 0.0004) \\ 0, \qquad \text{otherwise} \end{cases} \tag{6}$$

$$f_1(r) = -0.13767 r^2 + 1.0743 r + 0.1452 \tag{7}$$

$$f_2(r) = -0.776 r^2 + 0.5601 r + 0.1766 \tag{8}$$

where $f_1(r)$ and $f_2(r)$ denotes the upper bound and lower bound of the yellow line shown in Fig. 5, respectively. If the parameter S=1, it indicates the region is determined as the face region. Fig. 6 illustrates the results of proceeding the skin color detection.

2.5. Erosion and Dilation

In the morphological image processing, two common operations which can eliminate the effect of noise and connect the broken foreground are erosion and dilation. Moreover, the effect of the noise can also be reduced by further combining of operations of erosion and dilation [11].

Erosion is an operation which shrinks objects in a binary image. Then, the definition of erosion of input binary image A by structure element B is defined as [5], [6]

$$A \Theta B = \{ z \,|\, (B)_z \cap A^c \neq \varnothing \} \tag{9}$$

where $(B)_z$ denotes the translation of set B by point $z = (z_1, z_2)$, A^c is the set of all pixel coordinates

(a) (b)

Fig. 7 An example of erosion (a) Original image; (b) Eroded image.

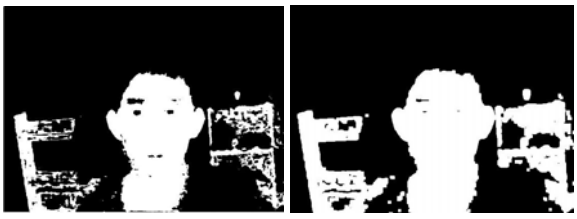

(a) (b)

Fig. 8 An example of dilation (a) Original image; (b) Dilated image.

that don't belong to set A, and $\varnothing$ is the empty set. Fig. 7(a) shows the original binary image, and Fig. 7(b) illustrates the resulting image with the operation of erosion. Similarly, dilation is an operation which thickens objects in a binary image and the dilation of A by B is defined in terms of set operations, such that [5], [6]

$$A \oplus B = \{ z \,|\, (\hat{B})_z \cap A \neq \varnothing \} \tag{10}$$

where $\hat{B}$ is the reflection of set B. Fig. 8(a) and (b) shows the original binary image and the dilated image, respectively.

3. Study and Design Procedures

In this paper, we mainly achieve the purpose of face recognition applications in numerology analysis by simply using a camera and some image processing techniques. Therefore, the design procedures which specify how to perform the extraction and recognition of each facial feature, such as eyes, eyebrows, mouth, and face shape are interpreted in detail in this section.

3.1. Face Extraction

In order to extract the face conveniently, the proposed system provides a system interface as shown in Fig. 9. After pressing the lower-left button "Take a picture", the face image will be extracted and displayed in the upper-right box. Moreover, the extracted face image will be saved as JPEG format and used for the numerology analysis in the future. The analysis results will be

Fig. 9 Interface of numerology analysis system.

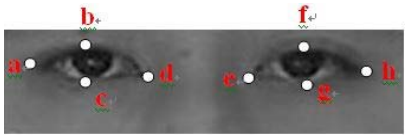

Fig. 10 Feature points of eyes.

shown in another interface by clicking the lower-right button "Announce the fate".

3.2. Eye Feature Extraction

Fig. 10 illustrates the resulting feature points of eyes after we perform the fundamental morphological operations presented in Section 2, such as the operations of the histogram, binary and erosion on the original image. Then, the parameters of eye feature which are used for the estimation of eye shape, such as the angle of elevation of the eye shape Ang_{eye}, the proportion of eye POE, and the proportion between the inner corner of the eye and outer corner of the eye $POIOE$ are given by

$$Ang_{eye} = \sin^{-1}\frac{D_{ady}}{D_{ad}} \tag{11}$$

$$POE = \frac{D_{ad}}{D_{bc}} \tag{12}$$

and

$$POIOE = \frac{D_{eq}}{D_{gr}} \tag{13}$$

where D_{ady} denotes the distance in y-axis between the inner corner of the eye and outer corner of the eye, D_{ad} denotes the distance between the inner corner of the eye and outer corner of the eye (i.e., the distance between point a and point d.), D_{de} denotes the distance between two inner corners of the eye (i.e., the distance between point d and point e), D_{bc} denotes the height of the eye (i.e., the distance between point b and point c), and D_{ah} between two outer corners of the eye (i.e., the distance between point a and point h).

According to Eqs. (11)-(13), the estimation parameters TSA and TSB can be obtained as

$$TSA = 20 \times POE^2 \tag{14}$$

$$TSB = 20 \times POIOE^2 \tag{15}$$

TABLE 1 CLASSIFICATION OF EYE FEATURE

Type	TSA	TSB	Ang_{eye}
Big Eyes	180~240	>140	-
Small Eyes	>240	<145	-
Round Eyes	<180	-	-
Upward-slanting Eyes	-	-	>10
Downward-slanting Eyes	-	-	<-5

Table 1 shows the classification of eye feature to define which eye shape the extracted image belongs to, based on the above both parameters TSA and TSB.

3.3. Eyebrow Feature Extraction

Similarly, we also need to obtain the feature points of eyebrows before we estimate the original image. After performing the fundamental morphological operations presented in Section 2, such as the operations of the histogram, binary and erosion on the original image, we can obtain the resulting feature points of eyebrows as shown in Fig. 11. Then, the parameters of eyebrow feature which are used for the estimation of eyebrow shape, such as the distance between the interior point of the eyebrow and the tip of the eyebrow D_{jk} (i.e., the distance between point j and point k), the distance between two interior points of the eyebrows D_{kl}, the distance in x-axis between the interior point of the eyebrow and the tip of the eyebrow D_{jkx}, the height of the eyebrow D_{mn} and the length of the eyebrow D_{ik} can be obtained and then the angle of elevation of the eyebrow Ang_{brow} can be obtained as

$$Ang_{brow} = \cos^{-1}\frac{D_{jkx}}{D_{jk}} \tag{16}$$

According to the above-mentioned parameters, Table 2 summaries the classification of eyebrow shape feature to provide us the decision rules to determine which eyebrow shape the extracted image belongs to.

Fig. 11 Feature points of eyebrows.

TABLE 2 CLASSIFICATION OF EYEBROW FEATURE

Type	D_{kl}	D_{mn}	D_{ik}	Ang_{brow}
Word Eyebrows	<=30	-	-	-
Short Eyebrows	-	-	<=40	-
Rough Eyebrows	-	>12	-	-
Sharp Eyebrows	-	-	-	>=10
Thin Eyebrows	-	<=12	-	<10

3.4. Mouth Feature Extraction

With the use of the fundamental morphological operations presented in Section 2 on the original image, 5 feature points of the mouth are obtained as shown in Fig. 12. Then, the definitions of the proportion of the mouth *POM* and the angle of elevation of the mouth Ang_{mouth} are given by

$$POM = \frac{D_{os}}{D_{pr}} \tag{17}$$

$$Ang_{mouth} = \cos^{-1}\frac{D_{osx}}{D_{os}}, \tag{18}$$

where D_{os} denotes the length of the mouth (i.e., the distance between the point *o* and point *s*), D_{pr} denotes the height of the mouth (i.e., the distance between the point *p* and point *r*), and D_{osx} denotes the distance in *x*-axis between the point *o* and point *s*). Thus, the classification of the mouth feature is summarized in accordance with Eqn. (17) and (18) as Table 3, in which the resulting para meters of D_{os}, POM and Ang_{mouth} are provided to

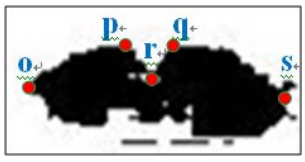

Fig. 12 Feature points of mouth.

TABLE 3 CLASSIFICATION OF MOUTH FEATURE

Type	D_{os}	POM	Ang_{mouth}
Wide Lips	>=65	-	-
Small Lips	<40	-	-
Oblique Lips	-	-	>=10
Full Lips	-	>=6	-
Thin Lips	-	<6	-

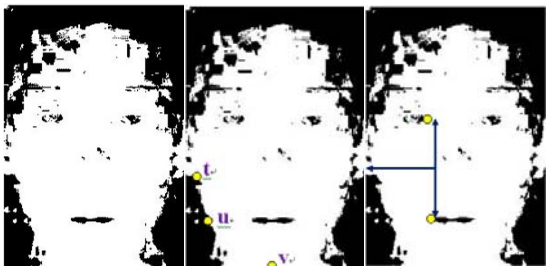

(a) (b) (c)

Fig. 13 (a) Extraced image after face detection; (b) Feature points *t*, *u*, and *v*; (c) Feature point *t*.

TABLE 4 CLASSIFICATION OF FACE FEATURE

Type	D_{tu}	Ang_{face}
Oblong Face	>=145	<=120
Square Face	<145	<=120
Triangular Face	-	>=160
Round Face	<120	-
Oval Face	>=120	-

determine which mouth shape the extracted image is.

3.5. Face Shape Feature Extraction

First, we perform the operation of face detection on the original image, thus the resulting image is shown as Fig. 13(a). Then, we can get the 3 feature points of the extracted image of the face (i.e., feature points *t*, *u*, and *v*) shown in Fig. 13(b). Moreover, Fig. 13(c) illustrates an example of how to get the feature point *t*, and it is note that the feature point *t* is assumed as the midpoint of the inner corner of the left eye and the left corner of the mouth. Therefore, we can obtain the parameter Ang_{face} and is given by

$$Ang_{face} = \cos^{-1}\frac{D_{tu}^2 + D_{uv}^2 - D_{tv}^2}{2D_{tu} \times D_{tv}} \tag{19}$$

where D_{tu} denotes the distance between the point *t* and point *u*, D_{uv} denotes the distance between the point *u* and point *v*, and D_{tv} denotes the distance between the point *t* and point *v*. As shown in Table 4 is the classification of face feature. Similarly, we can determine which face shape the extracted image belongs to, based on the parameters D_{tu} and Ang_{face} in the table.

4. EXPERIMENT RESULTS

Fig. 14 illustrates the classification of physiognomy features, such as the eye shape, eyebrow shape, mouth shape and face shape, which are the

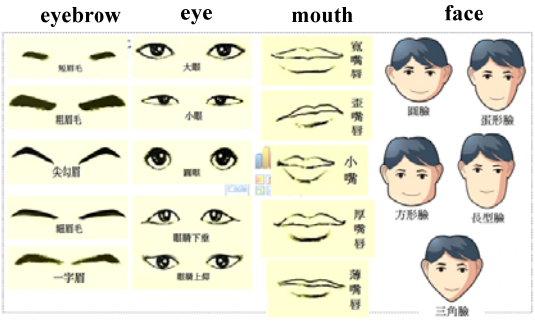

Fig. 14 Classifications of physiognomy features.

Fig. 15 An example of the experiment result.

important features and references generally used for the numerology analysis. Moreover, the interface of the proposed numerology analysis system is also shown in Fig. 15. First, the original image will be extracted via a camera and then displayed in the middle yellow box, after pressing the lower-left button "Take a picture". The results of numerology analysis will be demonstrated in the right box once we click the button "Announce the fate", based on the decision rule of each feature presented in Section 3. However, a decision or recognition error still occurs when we use the proposed system to perform the numerology analysis. The main reason is that the surrounding light is so bright or so dark that the average value of the pixel in the whole original image becomes raised or lowered, which results in the variance of the threshold.

5. Conclusions

In this paper, a facial numerology analysis system which utilizes image processing techniques instead of the traditional recognition by people was proposed. Our results showed that the proposed system can automatically and quickly provide the facial feature recognition and facial numerology analysis results by simply using a camera, MATLAB program and image processing techniques, which can improve the convenience and practicability of the analysis for the users indeed.

References

[1] S.-L. Chang, L.-S. Chen, Y.-C. Chung, and S.-W. Chen, "Automatic license plate recognition," *IEEE Trans. Intell. Transp. Syst.*, vol. 5, no. 1, pp. 42-53, Mar. 2004.

[2] F.-Z. Marcos, "Technological evaluation of two AFIS systems," *IEEE Aeros. Electron. Syst.*, vol. 20, no. 4, pp. 13-17, Apr. 2005.

[3] Q. Zhang and P. Shi, "Study on the medical image distributed dynamic processing method," *J. of Syst. Eng. and Electron.*, vol. 14, no. 4, pp. 69-76, Dec. 2003.

[4] A. Al-Qayedi and A.F. Clark, "An algorithm for face and facial-feature location based on grey-scale information and facial geometry," *7th Int. Conf. on Image Process. and Its Applicat.*, vol. 2, no. 465, pp. 625-629, Jul. 1999.

[5] R.C. Gonzalez, R.E. Woods and S.L. Eddins, *Digital Image Processing Using MATLAB*, New Jersey: Pearson Prentice Hall, 2004.

[6] A.M. Andrew, J.-H. Wang and C.-S. Tseng, *Introduction To Digital Image Processing Using MATLAB*, Taipei Taiwan: Cengage Learning, 2010.

[7] Y.-C. Chang, "RGB calibration for color image analysis in machine vision," *IEEE Trans. Image Process.*, vol. 5, no. 10, pp. 1414-1422, Oct. 1996.

[8] R.L.D. Queiroz, and K.M. Braun, "Color to gray and back: Color embedding into textured gray images," *IEEE Trans. Image Process.*, vol. 15, no. 6, pp. 1464-1470, June 2006.

[9] N. Otsu, "A threshold selection method from gray-level histograms," *IEEE Trans. Syst. Man Cybern.*, vol. 9, no. 1, pp. 62–66, Jan. 1979.

[10] C.-M. Tsai and H.-J. Lee, "Binarization of color document images via luminance and saturation color features," *IEEE Trans. Image Process.*, vol. 11, no. 4, pp. 434-451, Apr. 2002.

[11] M.-F. Huang, "*The study of monitoring* and *control system using human face tracking methods*," M.S. thesis, Electron. Eng., Nat. Cheng Kung Univ., Tainan, Taiwan, June 2003.

[12] M.-W. Wu, "*Automatic facial expression* analysis *system*," M.S. thesis, Inform. Eng., Nat. Cheng Kung Univ., Tainan, Taiwan, June 2003.